Rapid Quantification of Low Level Polymorph Content in a Solid Dose Form using Transmission Raman Spectroscopy

Julia. A. Griffen[a*], Andrew. W. Owen[a], Jonathan Burley[b], Vincenzo Taresco[b], Pavel Matousek[a,c]

[a] Cobalt Light Systems Ltd., Milton Park, Abingdon, OX14 4SD, UK

[b] Department of Pharmacy, University of Nottingham, Nottingham, NG7 2RD, UK

[c] Central Laser Facility, STFC Rutherford Appleton Laboratory, Harwell Campus, OX11 0QX, UK

*Corresponding Author

Abstract

This proof of concept study demonstrates the application of transmission Raman spectroscopy (TRS) to the non-invasive and non-destructive quantification of low levels (0.62 – 1.32 %w/w) of an active pharmaceutical ingredient's polymorphic forms in a pharmaceutical formulation. Partial least squares calibration models were validated with independent validation samples resulting in prediction RMSEP values of 0.03 – 0.05 % w/w and a limit of detection of 0.1 – 0.2 % w/w. The study further demonstrates the ability of TRS to quantify all tablet constituents in one single measurement. By analysis of degraded stability samples, sole transformation between polymorphic forms was observed while excipient levels remained constant. Additionally, a beam enhancer device was used to enhance laser coupling to the sample, which allowed comparable prediction performance at 60 times faster rates (0.2 s) than in standard mode.

1. Introduction

Rapid, non-invasive and non-destructive quantification of tablet or capsule constituents requiring no sample preparation is an important analytical area in pharmaceutical manufacturing. This requirement is driven by the limitations of existing technologies, often chromatographic based methods such as high performance liquid chromatography (HPLC), which, by their nature, are destructive techniques, require consumables, and takes significant time in use and maintenance.

An area of particular interest and high relevance to pharmaceutical applications is the quantification or identification of specific polymorphic forms of an active pharmaceutical ingredient (API) in a final dosage form. The necessity to quantify polymorphic forms often falls into two main areas. Firstly, from a commercial standpoint e.g. patent infringement, a patent may protect only one particular drug form. Secondly, efficacy assurance since the solubility (a function of polymorphic form) of the specific drug form will affect the bioavailability of the API.

The current technologies available for polymorph quantification are necessarily solid state as chromatographic techniques dissolve the sample and consequently destroy the crystallinity. Techniques such as X-ray diffraction (XRD), solid-state nuclear magnetic resonance (*ss*NMR), near-infrared and Raman spectroscopies have been widely studied and reviewed.[1–4]

A promising tool recently introduced into this area is transmission Raman spectroscopy.[5,6] The technique has seen numerous applications in pharmaceutical analysis, primarily focused around quantification of API in solid dose forms [7–10] recently gaining regulatory approval for batch release testing. [11]

The known advantages of Raman spectroscopy include high chemical specificity; the ability to quantify multiple constituents of a solid dose form,[12] the ability to analyse

polymorphs and crystalline state[13]; the high speed of analysis (<1 second)[14]; the absence of sample preparation; the absence of solvents and/or consumables and the non-destructive nature of analysis compared with the traditional analytical techniques. TRS also exhibits these favourable characteristics with the additional benefit, compared to a traditional backscatter geometry, of robustness against subsampling due to its high bulk sampling capability of the transmission method.[15,16] TRS has also displayed reduced sensitivity to matrix effects such as particle size, compaction force and sample thickness compared to other spectroscopic methods (particularly NIR spectroscopy).[17] As such TRS promises to offer a compelling and effective test method for pharmaceutical manufacturing, especially in challenging area of low drug loadings (typically down to ~0.1 – 1 % w/w). The technique's limitations of note include: the inability to analyse uncomplexed ionic compounds (e.g. NaCl) and interference from fluorescence in cases where this overwhelms the Raman Signal.

The technique has been previously demonstrated in the area of quantification of polymorphic components in binary form, in simple mixtures ranging from $0 - 100\%$[13,18] and in pharmaceutical formulations containing 10%w/w drug load with Limit of Detection (LOD) of 0.6%w/w. [19]

In this study we show, for the first time, comprehensive quantification of *low level* polymorphic forms (0.62 – 1.32 % w/w), an area where alternative techniques are often inapplicable due to limited sensitivity. Additionally we show the benefits of a beam enhancing technology enabling speeds of up to 60 times faster (0.2 seconds total acquisition time) but with similar quantification performance.

2. Experimental

### 2.1. Materials

In this study, flufenamic acid (FA) polymorphic forms were used, as previously studied and considered to be bench stable. Flufenamic acid {Sigma-Aldrich, UK} forms I (FA I) and III (FA III) were prepared as previously described.[13] Excipients included Ac-Di-SoL® (croscarmellose sodium {FMC Biopolymer, UK}) and lactose monohydrate {Sigma-Aldrich, UK}. Forms I and III were independently dispensed as a 17% premix in lactose monohydrate to assist with the weighing of very small quantities.

These compounds were selected for their wide use within the pharmaceutical industries. Additional consideration was given to their characteristic Raman features, for example lactose is a good Raman scatterer whereas Ac-Di-Sol® lacks Raman features and is very fluorescent.

2.2. Formulation

Samples were prepared following a 12 point DoE design, Figure 1. The final %w/w for each constituent in each of the samples is shown in Table I.
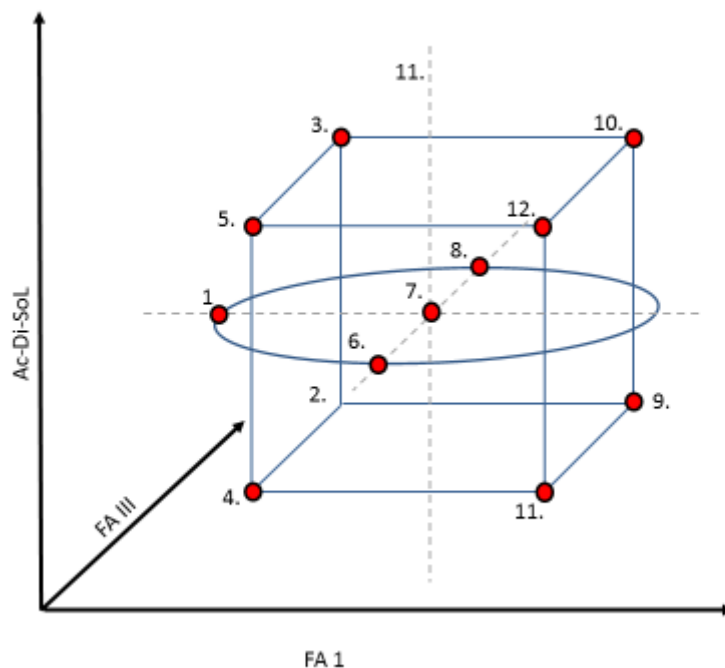
Figure 1: DoE central composite-type design schematically shown.

The centre point for each component is displayed in sample no. 7. Tablets were prepared by dispensing the weighed powder, total approx. 1.2g, into a pestle and mortar and grinding by hand. The mixed powder was then pressed into tablets weighing approx. 110 mg (103 – 115 mg range) and measuring approx. 2 mm (2.09 – 2.18 mm range) thick. From each sample 10 tablets were made. 8 were used for calibration and 2 were kept aside for stability testing. Centre point validation samples, triplicate dispensing of sample no.7, were made up independently with a new independent premix of FA polymorphs. Again, a total of 10 tablets were pressed per sample, 8 were used for calibration and 2 were kept aside for stability testing. A summary of samples and tablets (150 total) scanned are shown in Table II.

Stability samples were heated at 90 °C for 5 hours, in order to induce polymorphic transformation as has been previously demonstrated. [20]

Table I: formulation and content of each of the calibration and validation samples. Values displayed in % w/w

composition

Sample	Form I	Form III	Ac-Di-Sol®	Lactose	Total API
1	0.62	0.93	20.01	78.44	1.55
2	0.77	1.25	15.76	82.22	2.02
3	0.78	1.23	24.09	73.90	2.01
4	0.81	0.82	24.23	74.13	1.64
5	0.77	0.80	15.82	82.61	1.57
6	0.98	1.32	19.79	77.91	2.30
7	0.98	1.05	20.03	77.94	2.03
8	0.96	0.71	20.05	78.27	1.68
9	1.17	1.25	15.35	82.23	2.42
10	1.19	1.23	24.24	73.34	2.42
11	1.20	0.82	15.62	82.35	2.02
12	1.20	0.83	24.09	73.88	2.03
VAL 1	0.98	1.00	19.85	78.17	1.98
VAL 2	0.98	0.98	20.06	77.98	1.96
VAL 3	0.98	0.99	19.95	78.07	1.97

Table II: Summary of tablets prepared

Samples	No. of sample points n	DOE Sample no.'s	Repeats per sample no. r	No of tablets per sample t	Total No. of tablets $n \times r \times t$
Calibration	12	1 to 12	1	8	**96**
Validation	1	7	3	8	**24**
Stability	12	1 to 12	1	2	**30**
	1	7	3		

2.3. Beam enhancer

A Beam enhancer ('photon diode') element has been described previously.[14,21] The element comprised a of 25 mm diameter Iridian (Ottawa, Canada) bandpass filter centred at 830 nm with a bandwidth of 2.2 nm (FWHM) and transmittance of >90% at the central wavelength.

The photon diode is in essence a 'unidirectional' mirror permitting the transfer of photons from one side and acting as a reflector for photons impacting on it from the other side. It is located in close proximity to the sample placed and is directly over the laser illumination zone to prevent the loss of diffusely scattered photons from the sample's surface. As this loss can be substantial (>90 % of photons can escape by this mechanism) its prevention leads to much higher coupling efficiency of laser photons into the sample and much higher transmission Raman intensities. [21]

2.4. Measurements

The tableted samples were analysed using a TRS100 (Cobalt Light Systems Ltd., Oxfordshire, UK) transmission Raman instrument. The device utilises an automated sample tray. The CCD detector (iDUS, Andor, UK) and spectrograph (Headwall, USA) combination collects spectra over the wavelength range of 50- 2500 cm^{-1}. Acquisition parameters included a 4 mm diameter laser illumination spot size, medium lens collection optics (collection area diameter of ~6 mm), 650 mW laser power (830 nm), 0.6 s exposure time × 20 accumulations (i.e. 12 s total acquisition time per sample) without the beam enhancer. Utilising the beam enhancing optics within the sample tray required a reduced laser power of 350 mW to avoid saturation and permitted using shorter acquisition times, 0.01 s × 20 (0.2 s in total per sample).

Spectral analysis and model building was performed using Solo software (Eigenvector, WA).

3. Results and Discussion

Raman spectra of the pure API FA I and FA III indicated distinctive regions where the two polymorphs displayed different vibrational modes in Figure 2; e.g. the five most intense peaks of FA I are at 249, 786, 1001, 1334, 1609 cm^{-1}, whereas FA III can be identified by peaks at 748, 998, 1050, 1295 and 1618 cm^{-1}.

Calibration spectra were scanned and analysed using partial least squares (PLS) quantitative modelling. Visualisation of the baselined and normalised spectra, Figure 3, this indicates subtle spectral variation, highlighting the importance of chemometric techniques when analysing very low doses.

Calibration models for both standard acquisition parameter and with the beam enhancer for each tablet constituent are each tablet constituent are shown in
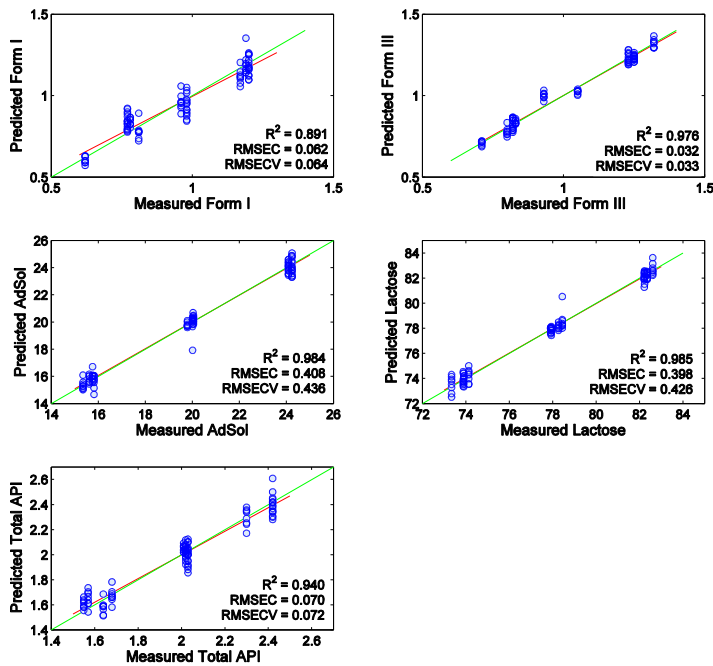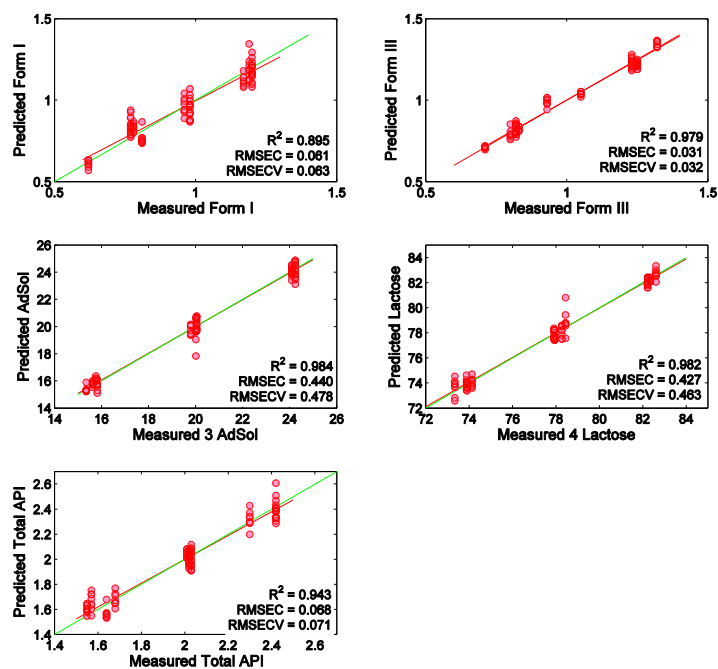
142   *Figure 4 and*

143   Figure 5. Model performance values are shown in Table III. Firstly notable is the similarity

144   of performance between Standard Acquisition values and Beam Enhancer values, with <

145   0.004 difference in the R^2 fit values and between 0.001 and 0.04 difference in root mean

146   square error of calibration/cross validation (RMSEC/CV). Linear fit values of $R^2 \approx 1.00$

147   indicate that all constituents could be modelled well. Lactose, Ac-Di-Sol and FA III models

148   perform similarly with R^2 values of ~ 0.98 compared to slightly lower values of ~0.89 for

149   FA I. Model performance of the FA calibration models are reflected in the RMSEC/CV

150   with a lower value being preferable. FA I calibration performs with slightly a higher value

151   of ~0.06 compared to better performing FA III with a value of ~0.03. Both display similar

152   values between RMSEC and CV indicating robustness of each calibration.

153   Model parameters were optimised to include 4 latent variables, pre-processing steps

154   comprised of baseline removal (Automatic Whittaker Filter), normalisation (Standard

155   normal variate scaling) and mean centring over the spectral range 200-1800 cm^{-1}. The latent

156   variables for the standard acquisition and beam enhancer calibration model, along with the

157   spectral difference of the FA I and FA III are shown in Figure 6. Latent variables for both

158 calibration models are comparable. The latent variables can be assigned as follows LV1and

159 LV2; contain features of FA I and FA III and lactose. LV3; is characteristic of peak

160 broadening and accounts differences between two polymorphic FA I and FA III forms.

161 LV4; displays a characteristic shape (spectral split of half up half down centred around

162 ~900 cm^{-1}) which is observed due to changes in thickness, which is more common in hand

163 made tablets.

164 Throughout model building various standard model parameters were tried and tested. These

165 settings used here were considered to be marginally better than others as they use a wide

166 spectral range, include all samples, and simple spectral pre-processing which follows good

167 working practices for PLS model building with Raman spectra.

168 *Table III: Calibration Model Performance [   ] Standard Acquisition [   ] Beam Enhancer*

	Form I	Form III	Ac-Di-SoL®	Lactose	Total API
R^2	0.891	0.976	0.984	0.985	0.940
	0.895	0.979	0.984	0.982	0.943
RMSEC	0.062	0.032	0.408	0.398	0.070
	0.061	0.031	0.440	0.427	0.068
RMSECV	0.064	0.033	0.436	0.426	0.072
	0.063	0.032	0.478	0.463	0.071

169

Validation centre points tablets were then scanned using the same acquisition parameters as the calibration, without and

171 *with the beam enhancer, and analysed (see*
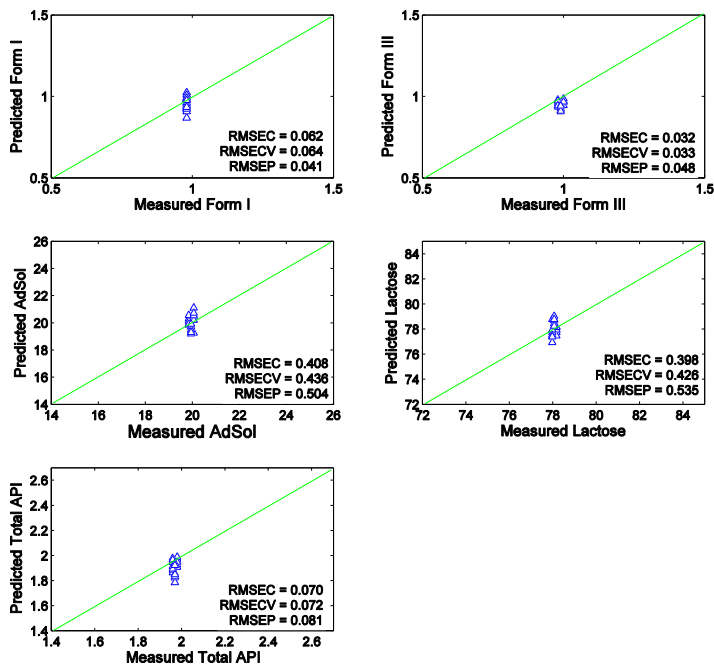

172
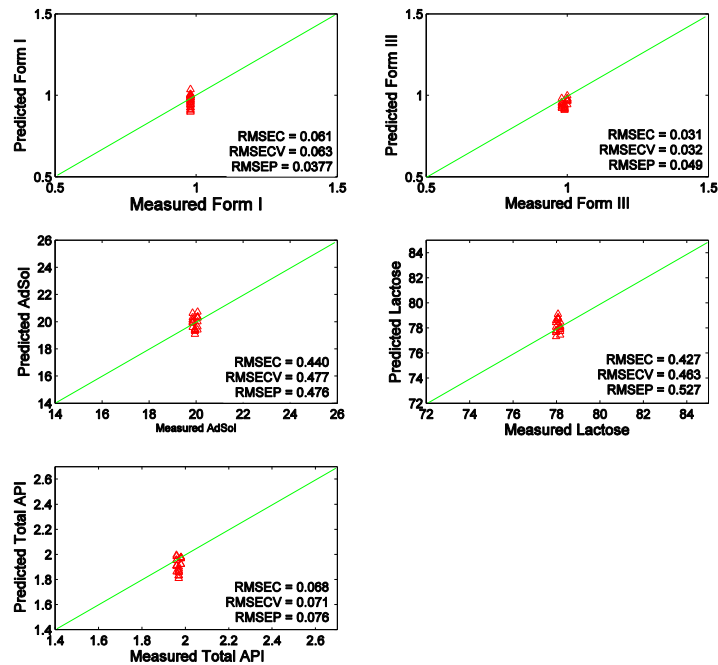
173   Figure 7and

174   Figure 8).

175 Prediction statistics and root mean square error of prediction (RMSEP), are shown in Table

176 IV. These uncertainty values of 0.05 translate to and uncertainty of +/- 0.05% w/w on any

177 prediction, which on a 1% nominal concentration results in a prediction window of 0.95 –

178 1.05 % w/w.

179 Stability samples were then scanned using the same acquisition parameters as the

180 calibration and analysed and predicted using the PLS calibration models previously

181 generated.   Predictions   are   shown   in
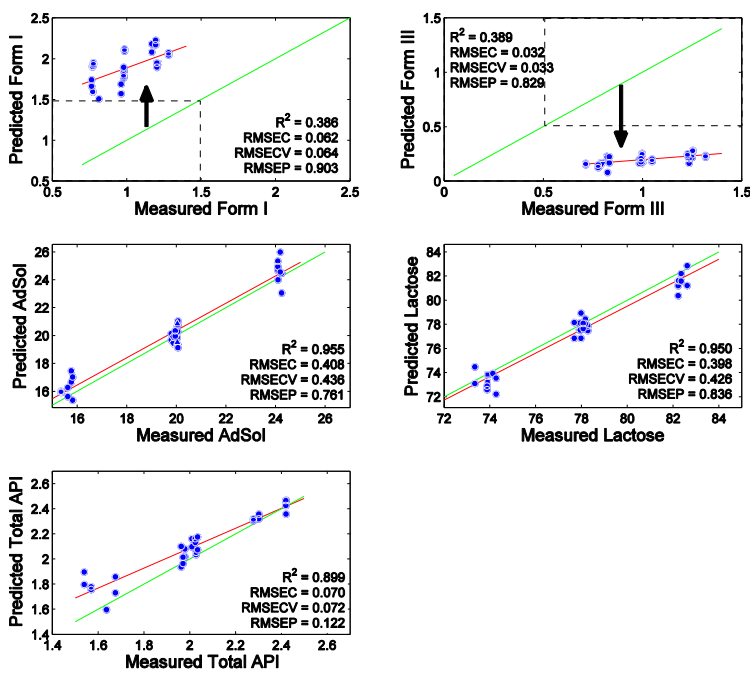
182
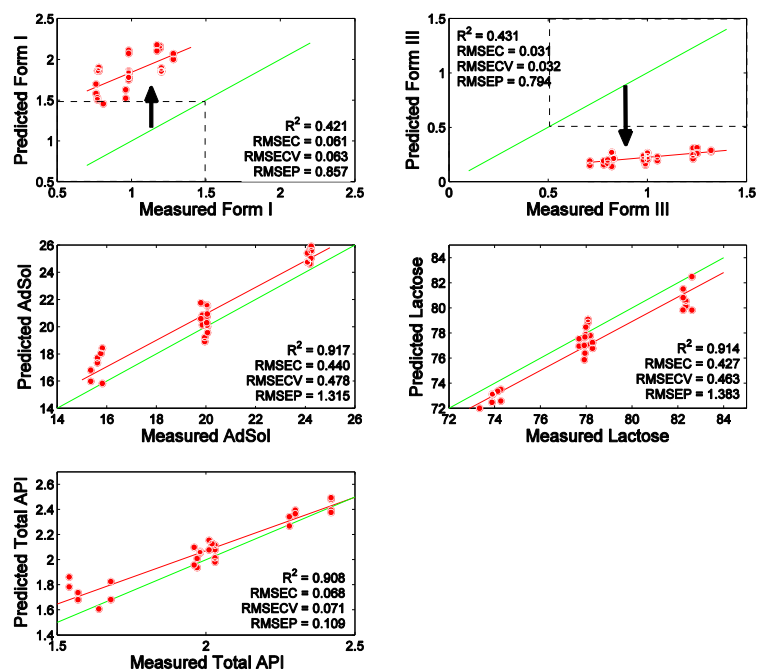
183 Figure 9 and

184 Figure 10. The results, prediction statistics, are summarised in

185 Table V.

186 The stability samples PLS predictions indicate an increase in the prediction of FA I and a

187 decrease in FA III from the original dispensed/calibration value. The total API predictions

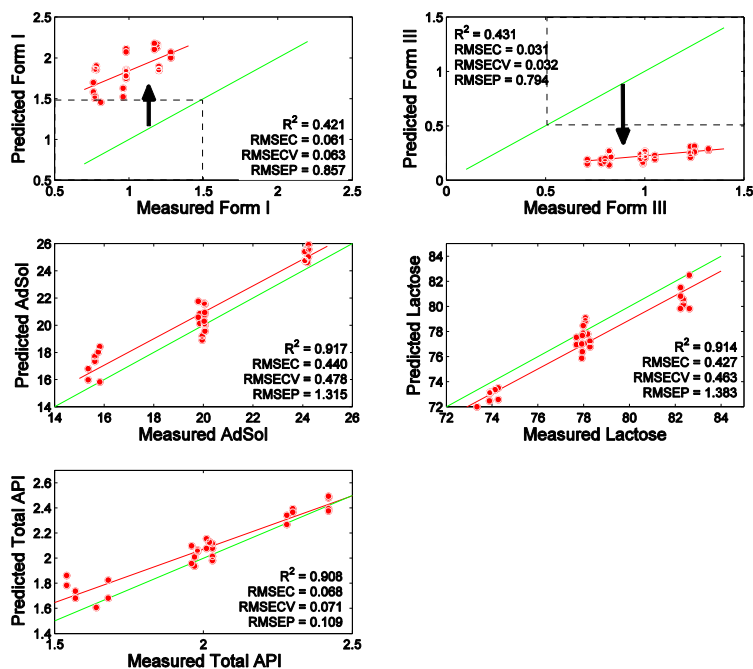188 remain consistent. This change in the samples was caused by heating of the tablet samples

189 at 90 °C for 5 hours. The observed predictions fits with the previous knowledge that on

190 heating FA III, if seeded, readily converts to FA I. [20]

From the sub plots displaying the PLS predictions of the stability samples, shown in
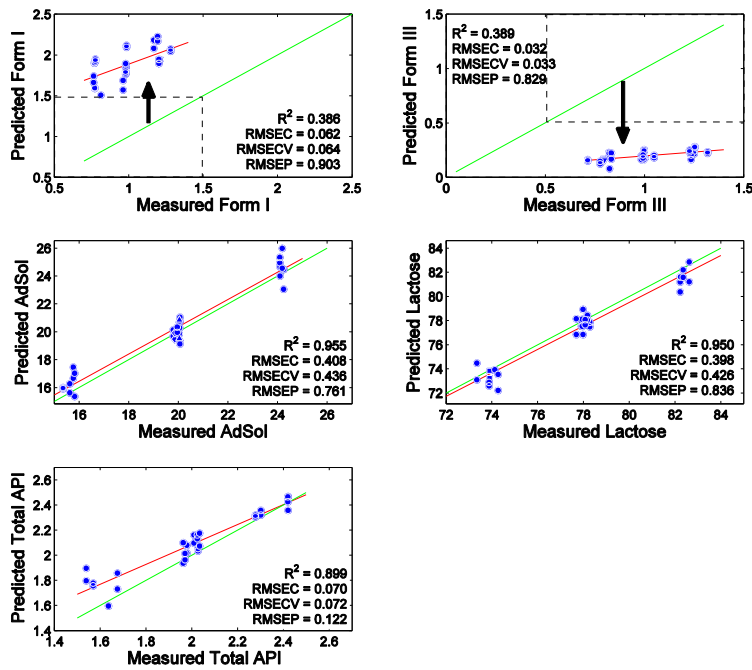
192

193 *Figure 9 and*

194 Figure 10, we observe consistency in predictions of the excipients before and after heating.

195 This observation suggests that these stability conditions only affect conversion of FA III to

196 FA I while the excipient content remains consistent.

197 Overall we see an increase in RMSEP values for the stability samples (Table IV) compared

198 to the centre point validation values (Table IV). This suggests that the heating has had an

199 effect on prediction performance. This could be due to the fact that the predictions are no

200 longer in the original calibration space (0.62 – 1.32 %w/w) for each of the polymorphic

201 forms, as marked by the dashed lines.

202 Interestingly within the stability sample predictions we observe a slight increase in the

203 RMSEP values in the prediction of the excipients with the use of the Beam Enhancer.

204 Previous work [22] has shown than the Beam Enhancer preferentially enhances the lower

205 surfaces of a sample. This suggests that on heating the surface of the tablet may appear

206 different than the bulk, hence we observe this slight difference in the excipient values.

207 *Additionally by measuring the total API content (see the last sub plot in*
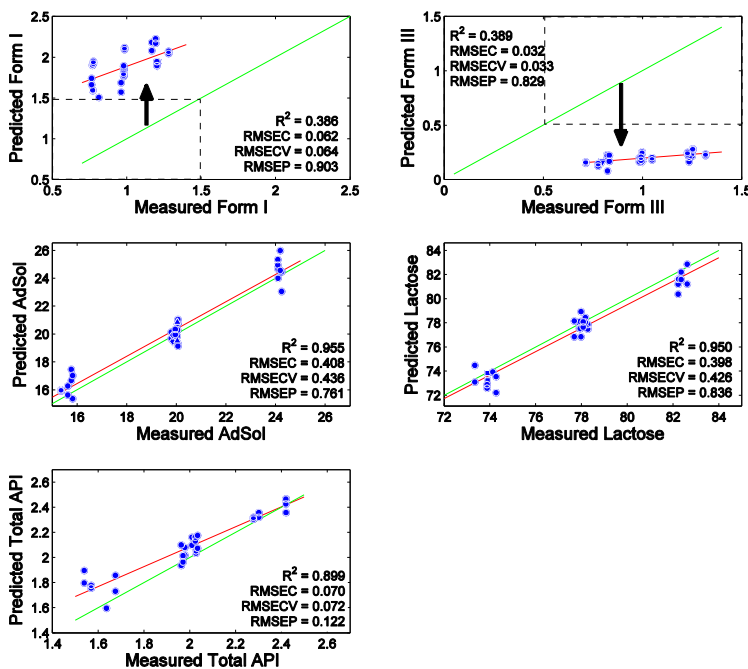
208
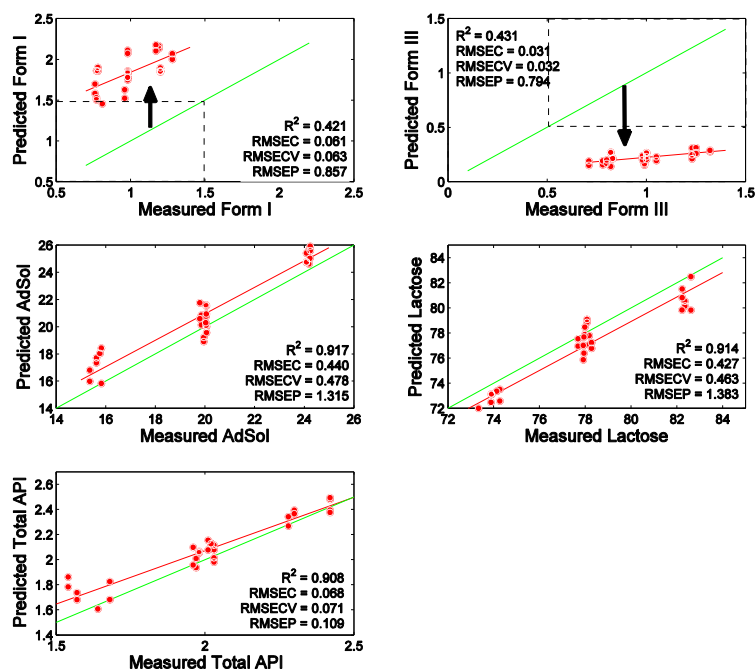
209 Figure 9 and

210 Figure 10) we can observe that this quantification is consistent, albeit with slight divergence

211 towards the lower total API content. Again this divergence could be attributed to the fact

212 that the predictions are no longer in the original calibration space (0.62 − 1.32 %w/w) for

213 each of the polymorphic forms, as marked by the dashed lines.

214

215 *Table IV: Centre point Validation Model Performance [   ] Standard Acquisition [   ] Beam Enhancer*

	Form I	Form III	Ac-Di-SoL®	Lactose	Total API
RMSEP	0.041	0.048	0.504	0.535	0.081
	0.037	0.049	0.476	0.527	0.076

216

217

218 *Table V: Stability Samples Model Performance [   ] Standard Acquisition [   ] Beam Enhancer*

	Form I	Form III	Ac-Di-SoL®	Lactose	Total API

RMSEP	0.903	0.829	0.761	0.836	0.122
	0.857	0.794	1.315	1.383	0.109

Limit of detection values, shown in

Table VI, were estimated from the quantitative models following ICH guidelines on

validation of analytical procedures where the detection limit may be expressed as:[23]

$$LOD = \frac{3.3\sigma}{S}$$

σ = standard deviation of the residual error of a regression

S = slope of the calibration curve.

Table VI: Limit of Detection values [   ] Standard Acquisition [   ] Beam Enhancer

	Form I	Form III	Ac-Di-SoL®	Lactose	Total API
LOD	0.23	0.11	1.45	1.43	0.25
	0.22	0.11	1.60	1.55	0.24

4. Conclusion

It has been demonstrated that transmission Raman spectroscopy has the ability to quantify

low levels (0.62 – 1.32 %w/w) of polymorphic forms of an API in intact tablets. The

quantitative model has been validated with independent centre point samples, displaying

239   satisfactory prediction and model statistics, with a RMSEP between +/- 0.04 to 0.05 % w/w

240   uncertainty on predicted values. The limit of detection was determined to be $0.1 - 0.2$ %

241   w/w. Additionally, we have demonstrated the ability to simultaneously quantify both API

242   and the excipients within the formulation. The ability to quantify excipients with little

243   additional effort demonstrates the selectivity possible with transmission Raman and has

244   practical benefits in terms of process understanding and control. This has been achieved

245   through the application of an efficient central composite DoE, Figure 1.

246   Stability investigations displayed the expected transformation of the API FA III to FA I.

247   Analysis of total API content indicated no significant degradation or loss of the API,

248   indicating direct conversion. Quantification of excipients within the stability samples

249   remained reasonable, indicating that the stability testing purely affected the API.

250

251   Finally the use of beam enhancer technology was investigated in order to reduce the data

252   acquisition time by a factor of 60. It has been demonstrated that there is no significant

253   detriment in either calibration model performance or prediction of unknown samples (centre

254   point or stability) when the beam enhancer technology is used in this application.

255

256   Overall this work shows that transmission Raman spectroscopy as a suitable tool for

257   analysis of low level polymorphic content in final pharmaceutical forms in a rapid manner.

258   These features would make transmission Raman spectroscopy a suitable technology for at-

259   line and/or real-time release and testing.

5. References

260

261

262 [1] T.L. Threlfall, Analysis of organic polymorphs. A review, Analyst. 120 (1995) 2435–2460.

263 doi:10.1039/an9952002435.

264 [2] D.E. Bugay, Characterization of the solid-state: spectroscopic techniques, Adv. Drug Deliv.

265 Rev. 48 (2001) 43–65. doi:10.1016/S0169-409X(01)00101-6.

266 [3] A. Siddiqui, Z. Rahman, V.A. Sayeed, M.A. Khan, Chemometric evaluation of near infrared,

267 fourier transform infrared, and Raman spectroscopic models for the prediction of nimodipine

268 polymorphs., J. Pharm. Sci. 102 (2013) 4024–35. doi:10.1002/jps.23712.

269 [4] A. Kumar, L. Joseph, J. Griffen, W. Jenny, T. Chi. Y, J. Hau, et al., Fast Non-Destructive

270 Detection of Low Level Crystalline Forms in Amorphous Spray Dried Dispersion Using

271 Transmission Raman Spectroscopy and Comparison to Solid-State NMR Spectroscopy, Am.

272 Pharmacetical Rev. (2016).

273 [5] B. Schrader, G. Bergmann, Die Intensitat des Ramanspektrums polykristalliner Substanzen,

274 Fresenius' Zeitschrift Fur Anal. Chemie. 225 (1967) 230–247. doi:10.1007/BF00983673.

275 [6] P. Matousek, a W. Parker, Bulk Raman Analysis of Pharmaceutical Tablets, Appl.

276 Spectrosc. 60 (2006) 1353–1357.

277 [7] J. Johansson, A. Sparén, O. Svensson, S. Folestad, M. Claybourn, Quantitative transmission

278 raman spectroscopy of pharmaceutical tablets and capsules, Appl. Spectrosc. 61 (2007)

279 1211–1218. doi:10.1366/000370207782597085.

280 [8] C. Eliasson, N. a. Macleod, L.C. Jayes, F.C. Clarke, S. V. Hammond, M.R. Smith, et al.,

281 Non-invasive quantitative assessment of the content of pharmaceutical capsules using

282 transmission Raman spectroscopy, J. Pharm. Biomed. Anal. 47 (2008) 221–229.

283 doi:10.1016/j.jpba.2008.01.013.

284 [9] M.D. Hargreaves, N. a. Macleod, M.R. Smith, D. Andrews, S. V. Hammond, P. Matousek,

285 Characterisation of transmission Raman spectroscopy for rapid quantitative analysis of intact

286 multi-component pharmaceutical capsules, J. Pharm. Biomed. Anal. 54 (2011) 463–468.

287 doi:10.1016/j.jpba.2010.09.015.

288 [10] M. Fransson, J. Johansson, A. Sparén, O. Svensson, Comparison of multivariate methods for

289   quantitative determination with transmission Raman spectroscopy in pharmaceutical

290   formulations, J. Chemom. 24 (2010) 674–680. doi:10.1002/cem.1330.

291 [11] J. Villaumie, H. Jeffreys, Revolutionising Raman with the transmission technique, Eur.

292   Pharm. Rev. 20 (2015) 41 – 45.

293   http://www.europeanpharmaceuticalreview.com/33080/topics/raman-

294   spectroscopy/revolutionising-raman-with-the-transmission-technique/ (accessed January 6,

295   2016).

296 [12] J. Griffen, A.W. Owen, P. Matousek, Comprehensive quantification of tablets with multiple

297   active pharmaceutical ingredients using transmission Raman spectroscopy—A proof of

298   concept study, J. Pharm. Biomed. Anal. 115 (2015) 277–282.

299   doi:10.1016/j.jpba.2015.07.019.

300 [13] A. Aina, M.D. Hargreaves, P. Matousek, J.C. Burley, Transmission Raman spectroscopy as a

301   tool for quantifying polymorphic content of pharmaceutical formulations., Analyst. 135

302   (2010) 2328–2333. doi:10.1039/c0an00352b.

303 [14] J. Griffen, A.W. Owen, P. Matousek, Development of Transmission Raman Spectroscopy

304   towards the in line, high throughput and non-destructive quantitative analysis of

305   pharmaceutical solid oral dose., Analyst. 140 (2015) 107–112. doi:10.1039/c4an01798f.

306 [15] A. Paudel, D. Raijada, J. Rantanen, Raman spectroscopy in pharmaceutical product design,

307   Adv. Drug Deliv. Rev. 89 (2015) 3–20. doi:10.1016/j.addr.2015.04.003.

308 [16] K. Buckley, P. Matousek, Recent advances in the application of transmission Raman

309   spectroscopy to pharmaceutical analysis, J. Pharm. Biomed. Anal. 55 (2011) 645–652.

310   doi:10.1016/j.jpba.2010.10.029.

311 [17] A. Sparén, M. Hartman, M. Fransson, J. Johansson, O. Svensson, Matrix Effects in

312   Quantitative Assessment of Pharmaceutical Tablets Using Transmission Raman and Near-

313   Infrared (NIR) Spectroscopy, Appl. Spectrosc. 69 (2015) 580–589. doi:10.1366/14-07645.

314 [18] C. McGoverin, M.D. Hargreaves, P. Matousek, K.C. Gordon, Pharmaceutical polymoprh

315   quantified with tranmission Raman spectrscopy, J. Raman Spectrosc. 43 (2012) 280–285.

316 [19] M.C. Hennigan, A.G. Ryder, Quantitative polymorph contaminant analysis in tablets using

317   Raman and near infra-red spectroscopies, J. Pharm. Biomed. Anal. 72 (2013) 163–171.

318   doi:10.1016/j.jpba.2012.10.002.

319 [20] V. López-Mejías, J.W. Kampf, A.J. Matzger, Nonamorphism in flufenamic acid and a new

320   record for a polymorphic compound with solved structures., J. Am. Chem. Soc. 134 (2012)

321   9872–5. doi:10.1021/ja302601f.

322 [21] P. Matousek, Raman signal enhancement in deep spectroscopy of turbid media, Appl.

323   Spectrosc. 61 (2007) 845–854. doi:10.1366/000370207781540178.

324 [22] Y. Zhang, G. McGeorge, Quantitative Analysis of Pharmaceutical Bilayer Tablets Using

325   Transmission Raman Spectroscopy, J. Pharm. Innov. (2015). doi:10.1007/s12247-015-9223-

326   8.

327 [23] ICH, Validation of Analytical Procedures: text and methodolgy, 1996.

328 6. Figures

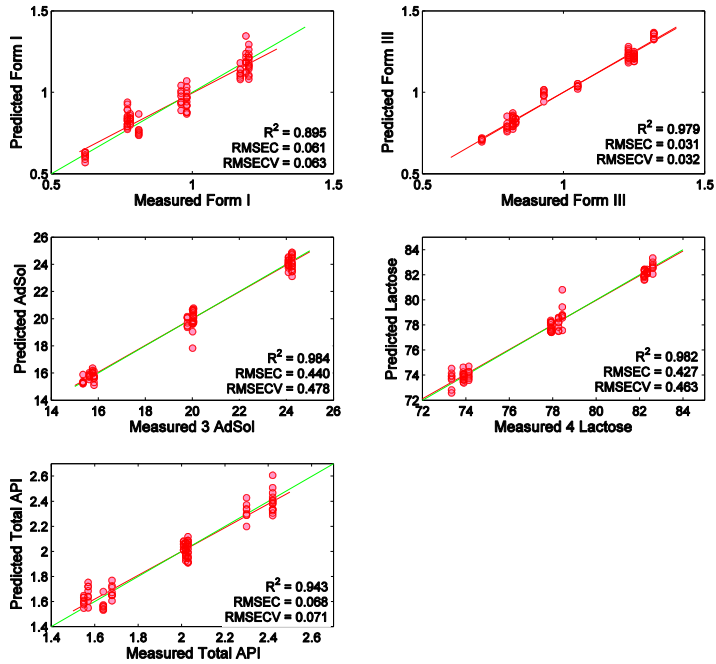329
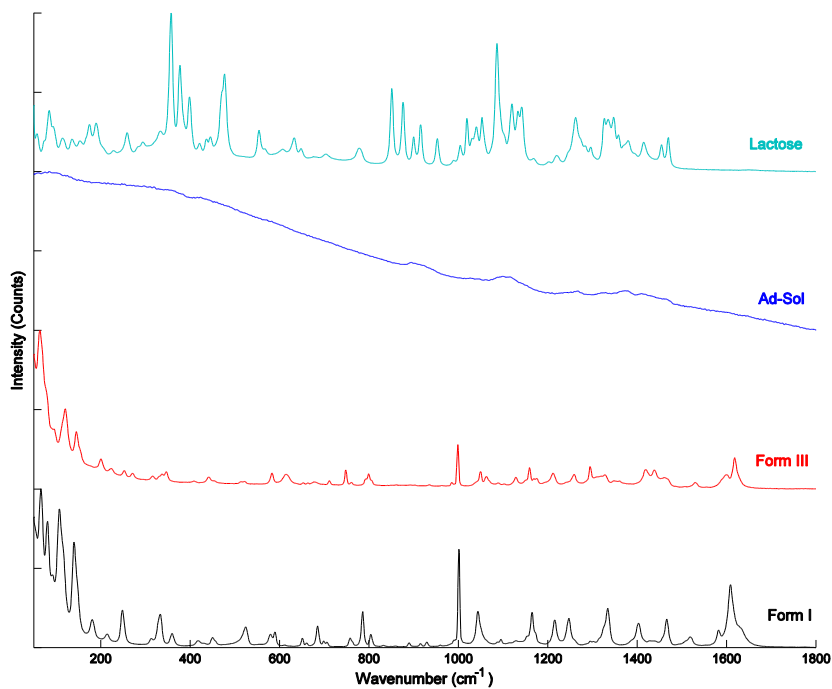
Figure 2: Raw individual component TRS spectra

331
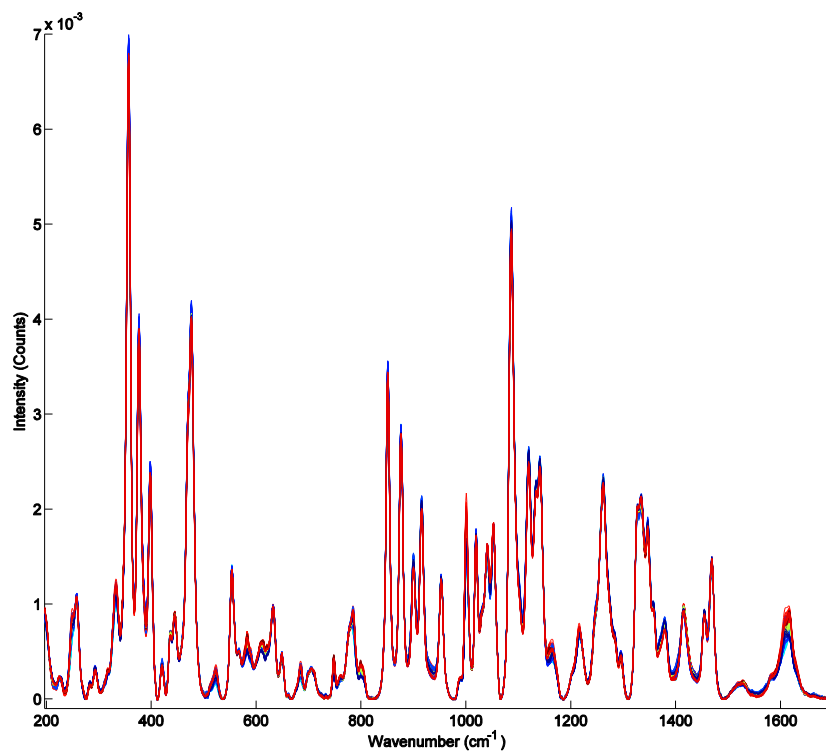
Figure 3: Calibration Spectra baseline subtracted and normalised coloured according to flufenamic acid type.
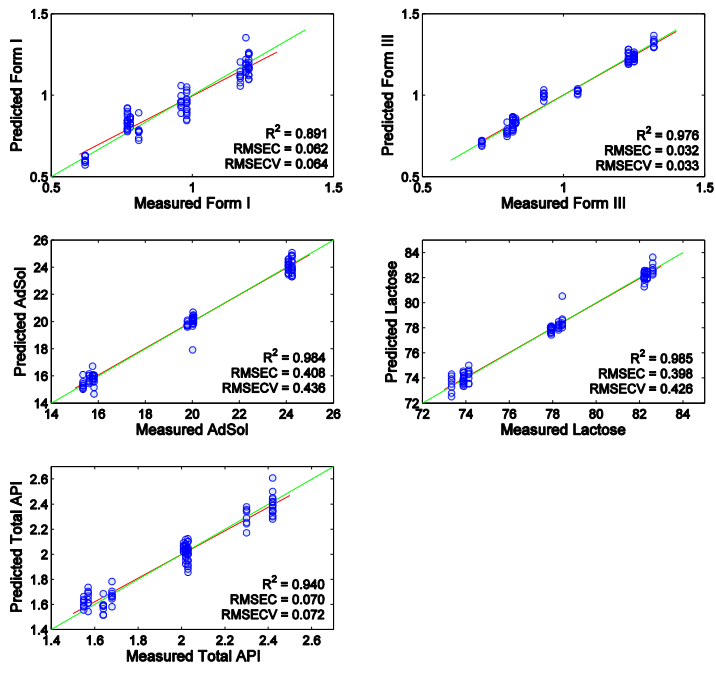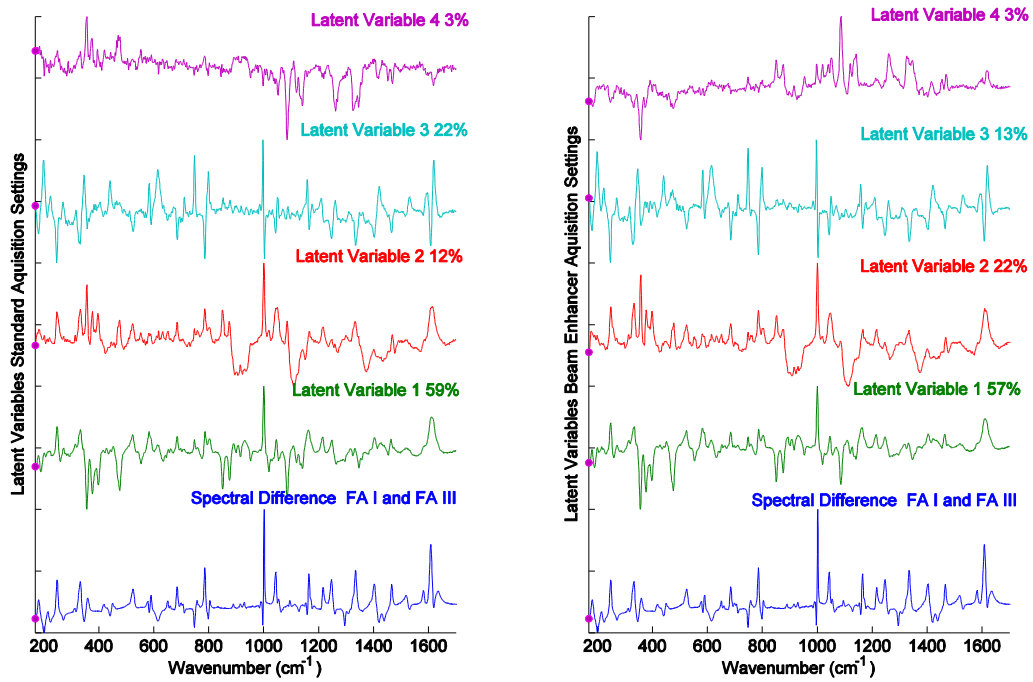
333

334   *Figure 4: Standard Acquisition Calibration*
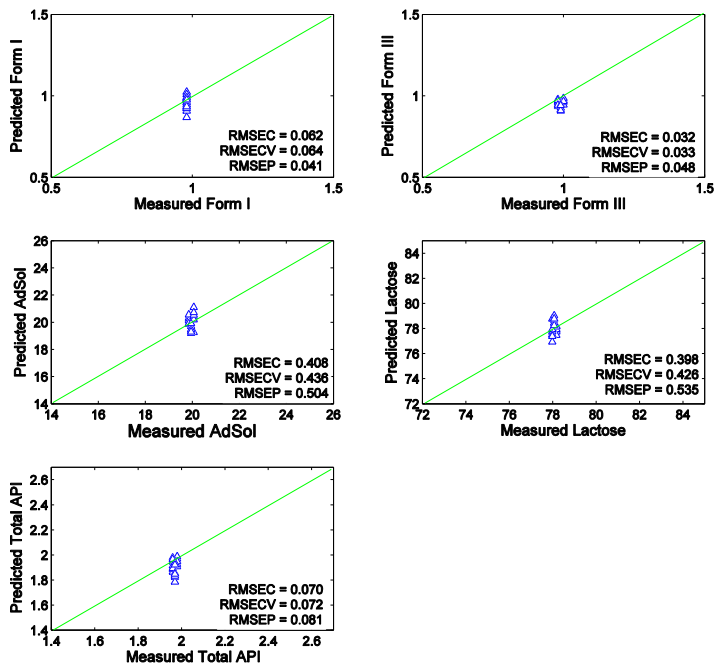

335

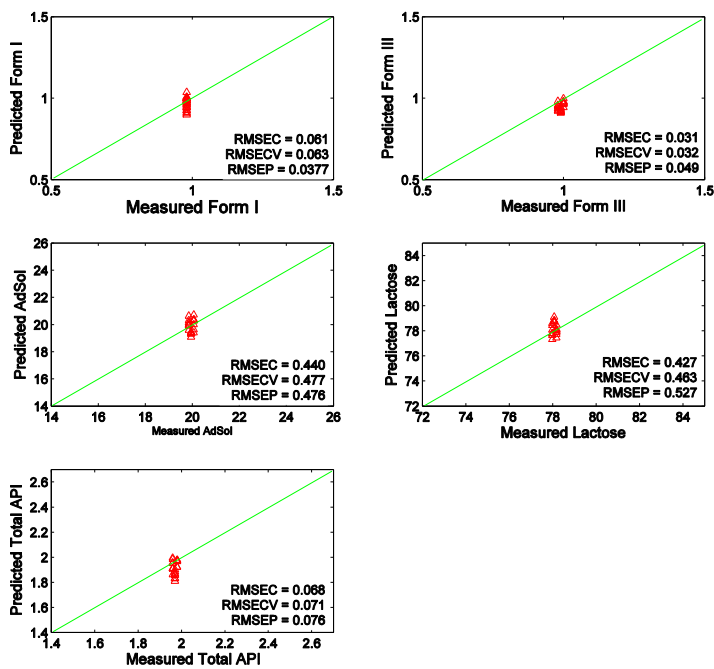336   *Figure 5: Beam Enhancer Calibration*

337

338   *Figure 6: Latent Variables for Standard Acquisition Models*
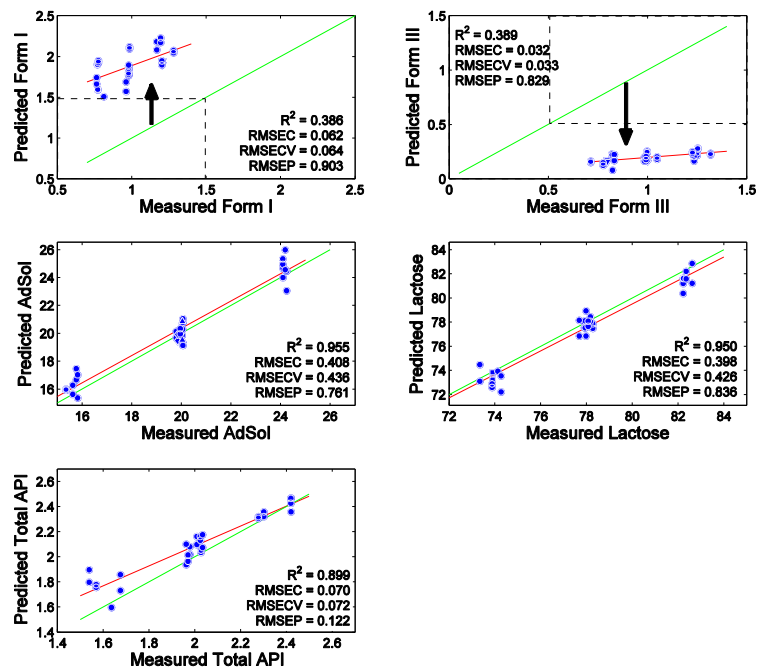

339

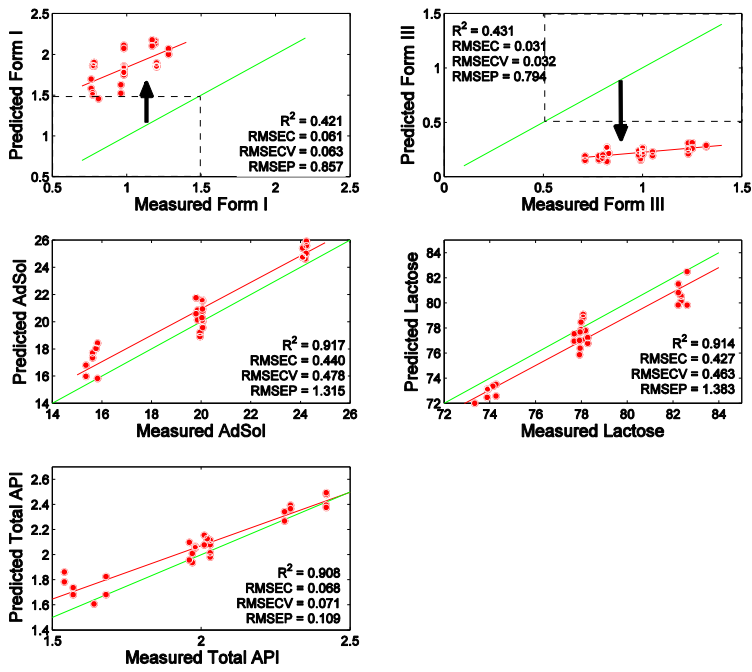340   *Figure 7: Standard Acquisition Validation*

Figure 8: Beam Enhancer Validation

Figure 9: Standard Acquisition Stability Samples

345

346 *Figure 10: Beam Enhancer Stability Samples*